Trajectory Tracking Control of an Autonomous Underwater Vehicle Using Lyapunov-Based Model Predictive Control

Chao Shen, *Member, IEEE*, Yang Shi, *Fellow, IEEE*, and Brad Buckham, *Member, IEEE*

***Abstract*—This paper studies the trajectory tracking control problem of an autonomous underwater vehicle (AUV). We develop a novel Lyapunov-based model predictive control (LMPC) framework for the AUV to utilize computational resource (online optimization) to improve the trajectory tracking performance. Within the LMPC framework, the practical constraints, such as actuator saturation, can be explicitly considered. Also, the thrust allocation subproblem can be addressed simultaneously with the LMPC controller design. Taking advantage of a nonlinear backstepping tracking control law, we construct the contraction constraint in the formulated LMPC problem so that the closed-loop stability is theoretically guaranteed. Sufficient conditions that ensure the recursive feasibility, and hence the closed-loop stability, are provided analytically. A guaranteed region of attraction is explicitly characterized. In the meantime, the robustness of the tracking control can be improved by the receding horizon implementation that is adopted in the LMPC control algorithm. Simulation results on the Saab SeaEye Falcon model AUV demonstrate the significantly enhance trajectory tracking control performance via the proposed LMPC method.**

***Index Terms*—Autonomous underwater vehicle (AUV), backstepping, Lyapunov-based nonlinear control, model predictive control (MPC), thrust allocation (TA), trajectory tracking.**

I. Introduction

THE autonomous underwater vehicles (AUVs) exemplify the recent advances in the marine robotics field and has been receiving a growing interest from both industry and academia due to their potential to substantially reduce risks and operational costs in various submarine projects [1]. The core feature of the AUV refers to the capability of reacting appropriately during the missions without intervention from human operators, which, on the other hand, justifies an elaborated control system [2]–[4].

The trajectory tracking is one fundamental functionality of the AUV control system, but is never an easy task. The highly nonlinear and cross-coupled system dynamics together with the unpredictable complex underwater environment, which introduces considerable disturbances and uncertainties challenges the controller design. There exist plenty of research studies in the literature devoted to the AUV trajectory tracking control. When the desired trajectory is piecewise linear (i.e., way-point tracking), the assumptions for local linearization can hold, and the classic linear control techniques are applied to solve the trajectory tracking problem [5]. The linear control methods, such as the proportional-integral-derivative (PID) and linear-quadratic-regulator are often preferred due to their easy implementation. However, linear control techniques will be no longer effective if the desired trajectory represents a curve in the workspace, because the curve trajectory, by nature, emphasizes the nonlinearity of the AUV motion. Therefore, the nonlinear control techniques are often resorted to for the tracking controller design. The Lyapunov-based backstepping control (BSC) represents the mainstream method for the AUV tracking control because the control law exploits those "good" nonlinearities in the system dynamics, which gains additional robustness compared to the inverse dynamics control (feedback linearization). Examples include [6] and [7]. In [6], the AUV trajectory tracking control considers the complete kinematics and dynamics of the motion and design the control law using the backstepping technique. An output feedback tracking control via Lyapunov-based backstepping can be found in [7]. Due to the insensitivity to model uncertainties, the sliding model control (SMC) becomes the other mainstream nonlinear method for the AUV trajectory tracking control. In [8], an enhanced trajectory tracking performance is obtained by the combining the SMC, PID, and robust control. To eliminate the main drawback associated with the SMC, known as the "chattering" effect, in [9], an adaptive law is incorporated in the control law design. In [10], the higher order sliding mode is used for the chattering-free trajectory tracking control. Most recent studies on autonomous vehicle tracking control try to address more practical issues [11]–[13]. The system constraints, such as thrust limit and safe operating area are inevitable in real AUV applications, hence, it is desired to consider these constraints in the tracking controller design.

Manuscript received June 19, 2017; revised September 6, 2017, and October 24, 2017; accepted November 5, 2017. Date of publication December 4, 2017; date of current version March 6, 2018. This work was supported in part by the Natural Sciences and Engineering Research Council of Canada, and in part by the National Natural Science Foundation of China under Grant 61473116. *(Corresponding author: Yang Shi)*

The authors are with the Department of Mechanical Engineering and the Institute for Integrated Energy Systems (IESVic), University of Victoria, Victoria, BC V8W 3P6, Canada (e-mail: shenchao@uvic.ca; yshi@uvic.ca; bbuckham@uvic.ca).

Color versions of one or more of the figures in this paper are available online at http://ieeexplore.ieee.org.

Digital Object Identifier 10.1109/TIE.2017.2779442

Model predictive control (MPC) is an optimization-based time-domain control method [14], [15]. Compared to most traditional control methods [16], [17], the distinct feature of MPC lies in its capability of systematically handling system constraints within the controller design. Therefore, MPC provides a powerful framework for solving all kinds of control engineering problems [18], [19]. In terms of AUV trajectory tracking control, in [20], the linear MPC solution is provided together with a genetic algorithm to solve the associated quadratic programming problem. The combined AUV motion control problem of path planning and trajectory tracking is resolved in [21] using nonlinear model predictive control (NMPC). In [22], the efficiency of solving the optimization problem associated with the NMPC tracking control is mainly focused. An ad hoc algorithm based on numerical continuation is exploited to speed up the online calculation. Another strategy aiming at reducing the online computation load of NMPC is reported in [23]. By decomposing the 6 DOF dynamic equations into three slightly interacted subsystems, the formulated NMPC problem can be solved in a distributed way. Nevertheless, since MPC determines the control signal by solving optimization problems, the control signal is an implicit function of the system state, which brings huge challenges in analyzing the closed-loop stability, especially for nonlinear systems, such as AUVs. The optimality of the solution does not indicate the closed-loop stability since a finite prediction horizon is used for practical implementation. To obtain this important property, the standard MPC design technique requires the employment of additional terminal constraints to the formulated optimization problem, and to construct an auxiliary stabilizing control law via local linearization [14]. However, as mentioned before, local linearization is inappropriate for the AUV trajectory tracking applications. The standard MPC design technique appears difficult to apply. Since stability is the most important property of any closed-loop control system and must be ensured, it is urgent to provide a means to guarantee closed-loop stability for optimization-based trajectory tracking control.

In this paper, we develop a novel Lyapunov-based nonlinear model predictive control (LMPC) scheme for AUVs to solve the trajectory tracking control problem. The LMPC can well handle the nonlinear and cross-coupled system dynamics and the system constraints in terms of thrust limits. It circumvents the local linearization that is needed by standard MPC [24] and guarantees the closed-loop stability in a relatively simple way. A LMPC-based tracking control algorithm is proposed. Within the LMPC algorithm, the thrust allocation (TA) subproblem, i.e., the coordination of thrusters to generate the matched generalized force and moment requested by the tracking control law, need not be solved separately as the thruster distribution can be directly formulated into the optimization problem. The Lyapunov-based backstepping technique is applied to construct a contraction constraint in the LMPC problem formulation, which theoretically guarantees the recursive feasibility and closed-loop stability of the proposed LMPC control algorithm.

The main contribution of this paper is three-fold as follows.

1) A novel LMPC algorithm is proposed to solve the AUV trajectory tracking control problem. With the proposed LMPC, the performance as well as the robustness of the tracking control can be significantly improved. Besides, the TA subproblem can be simultaneously addressed within the controller design.
2) The proposed LMPC framework circumvents the local linearization step that is difficult for trajectory tracking problems, but important in standard MPC control design. Sufficient conditions for recursive feasibility and closed-loop stability are explicitly derived. A guaranteed region of attraction (ROA) is characterized analytically.
3) For the LMPC tracking control, only the control performance (neither feasibility nor stability) is affected by the quality of the optimal solution. Therefore, the proposed LMPC essentially creates a tradeoff between computational complexity and control performance, which introduces an effective mechanism for the AUV to allocate the computing resources.

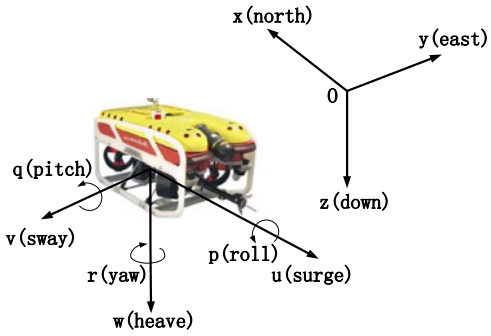

Fig. 1. Reference frames. (Falcon image courtesy of http://seaeye.com).

The rest of this paper is organized as follows. Section II introduces the AUV model and its important properties which are exploited in the following controller design. In Section III, the optimization problem formulation is introduced together with the LMPC algorithm. Section IV provides the stability analysis of the LMPC control with an auxiliary controller derived via the Lyapunov-based backstepping technique. Simulation results are demonstrated in Section V. Section VI gives some conclusive remarks.

Throughout the paper, the following notations are used: the column operation $[\rho_1^{\mathrm{T}}, \ldots, \rho_n^{\mathrm{T}}]^{\mathrm{T}}$ is denoted as $col(\rho_1, \ldots, \rho_n)$; the diagonal operation is denoted by $\mathrm{diag}(\cdot)$; the square of a weighted Euclidean norm $\rho^{\mathrm{T}} A \rho$ is abbreviated by $\|\rho\|_A^2$; and the infinity norm and 2 norm are denoted by $\|\cdot\|_\infty$ and $\|\cdot\|_2$, respectively. The symbol $\mathbf{1}$ is used to represent a column vector with all elements to be 1. The $\max\{\cdot\}$ is a function that returns the largest element within the brace. The absolute value operator applying on a vector $|\rho|$ takes the absolute value element-wisely.

II. Modeling

The experimental platform considered here is the Saab SeaEye Falcon shown in Fig. 1. Since the thruster layout does not allow active control on roll and pitch motion, we study the trajectory tracking control of the Falcon in the local level plane.

Two reference frames are introduced. The body reference frame (b-frame) is affixed to the vehicle with the origin selected to be the center of gravity. The motion of the vehicle, subsequently, is described as the motion of the b-frame with respect to the inertial reference frame (i-frame), which records the global information of the motion. Then, the AUV motion can be precisely described by the kinematic equations which deal with the coordinates transformation between the two frames, and the dynamic equations which analyze the cause of the motion.

The kinematic equations can be expressed in the following compact form [5]:

$$\dot{\boldsymbol{\eta}} = \mathbf{R}(\psi)\mathbf{v} \tag{1}$$

where $\boldsymbol{\eta} = [x, y, \psi]^{\mathrm{T}}$ denotes the position and heading of the AUV, represented in the i-frame; $\mathbf{v} = [u, v, r]^{\mathrm{T}}$ denotes the velocity of the vehicle, represented in the b-frame; $\mathbf{R}(\psi)$ is the rotation matrix depending on the heading ψ

$$\mathbf{R}(\psi) = \begin{bmatrix} \cos\psi & -\sin\psi & 0 \\ \sin\psi & \cos\psi & 0 \\ 0 & 0 & 1 \end{bmatrix}. \tag{2}$$

The dynamic equations are established via laws of Newton

$$\mathbf{M}\dot{\mathbf{v}} + \mathbf{C}(\mathbf{v})\mathbf{v} + \mathbf{D}(\mathbf{v})\mathbf{v} + \mathbf{g}(\boldsymbol{\eta}) = \boldsymbol{\tau} \tag{3}$$

where $\boldsymbol{\tau} = [F_u, F_v, F_r]^{\mathrm{T}}$ denotes the generalized thrust force. $\mathbf{M} = \mathrm{diag}(M_{\dot{u}}, M_{\dot{v}}, M_{\dot{r}})$ represents the inertia matrix including the added mass; $\mathbf{C}(\mathbf{v})$ denotes the Coriolis and centripetal matrix having the following form:

$$\mathbf{C}(\mathbf{v}) = \begin{bmatrix} 0 & 0 & -M_{\dot{v}}v \\ 0 & 0 & M_{\dot{u}}u \\ M_{\dot{v}}v & -M_{\dot{u}}u & 0 \end{bmatrix} \tag{4}$$

and $\mathbf{D}(\mathbf{v}) = \mathrm{diag}(X_u, Y_v, N_r) + \mathrm{diag}(D_u|u|, D_v|v|, D_r|r|)$ is the damping matrix; and $\mathbf{g}(\boldsymbol{\eta})$ represents the restoring force.

The generalized thrust force $\boldsymbol{\tau}$ is actually generated by four thrusters $\mathbf{u} = [u_1, u_2, u_3, u_4]^{\mathrm{T}}$ which follows $\boldsymbol{\tau} = \mathbf{B}(\boldsymbol{\alpha})\mathbf{u}$. Here, $\boldsymbol{\alpha}$ represents the azimuth vector of the thrusters represented in b-frame. For the Falcon, the azimuth angles are fixed. Therefore, we have the thrust distribution

$$\boldsymbol{\tau} = \mathbf{B}\mathbf{u} \tag{5}$$

where $\mathbf{B}$ is a constant input matrix.

Then, the dynamic model for the AUV trajectory tracking can be established by combining (1), (3), and (5)

$$\dot{\mathbf{x}} = \begin{bmatrix} \mathbf{R}(\psi)\mathbf{v} \\ \mathbf{M}^{-1}(\mathbf{B}\mathbf{u} - \mathbf{C}\mathbf{v} - \mathbf{D}\mathbf{v} - \mathbf{g}) \end{bmatrix} = \mathbf{f}(\mathbf{x}, \mathbf{u}) \tag{6}$$

where the state is defined as $\mathbf{x} = [x, y, \psi, u, v, r]^{\mathrm{T}}$ and the control as $\mathbf{u} = [u_1, u_2, u_3, u_4]^{\mathrm{T}}$.

The following important properties of the model are easily explored and will be exploited in the controller design.

- P-1: The initial matrix is symmetric positive definite and upper bounded: $\infty > \bar{m}\mathbf{I} \geq \mathbf{M} = \mathbf{M}^{\mathrm{T}} > 0$.
- P-2: The Coriolis and centripetal matrix is skew-symmetric: $\mathbf{C}(\mathbf{v}) = -\mathbf{C}^{\mathrm{T}}(\mathbf{v})$.
- P-3: The inverse of rotation matrix satisfies: $\mathbf{R}^{-1}(\psi) = \mathbf{R}^{\mathrm{T}}(\psi)$ and it preserves length $\|\mathbf{R}^{\mathrm{T}}(\psi)\dot{\boldsymbol{\eta}}\|_2 = \|\dot{\boldsymbol{\eta}}\|_2$.
- P-4: The damping matrix is positive definite: $\mathbf{D}(\mathbf{v}) > 0$.
- P-5: The input matrix satisfies that $\mathbf{B}^{\mathrm{T}}\mathbf{B}$ is nonsingular.
- P-6: The restoring force $\mathbf{g}(\boldsymbol{\eta})$ is bounded: $\|\mathbf{g}(\boldsymbol{\eta})\|_\infty \leq \bar{g}$.

III. LMPC-Based Trajectory Tracking Control

Consider a desired trajectory $p(t) = [x_d(t), y_d(t)]^{\mathrm{T}}$ which defines the position of the AUV in the local level plane. Here, we assume that the following conditions hold:

Assumption 1: The desired trajectory $p(t)$ together with its derivatives is smooth and bounded, satisfying that: $0 \leq \underline{p} \leq \|p(t)\|_\infty \leq \bar{p} < \infty$, $0 < \underline{p_1} \leq \|\dot{p}(t)\|_\infty \leq \bar{p}_1 < \infty$, $0 \leq \underline{p_2} \leq \|\ddot{p}(t)\|_\infty \leq \bar{p}_2 < \infty$, and $0 \leq \underline{p_3} \leq \|\dddot{p}(t)\|_\infty \leq \bar{p}_3 < \infty$.

We augment $p(t)$ to a reference system so that each state of the AUV system (6) has a feasible reference. Let $\mathbf{x}_d(t) = [x_d(t), y_d(t), \psi_d(t), u_d(t), v_d(t), r_d(t)]^{\mathrm{T}}$ with

$$\begin{aligned} \psi_d(t) &= \mathrm{atan2}(\dot{y}_d(t), \dot{x}_d(t)) \\ u_d(t) &= \sqrt{\dot{x}_d^2(t) + \dot{y}_d^2(t)} \\ v_d(t) &= 0 \\ r_d(t) &= (\dot{x}_d(t)\ddot{y}_d(t) - \dot{y}_d(t)\ddot{x}_d(t))/(\dot{x}_d^2(t) + \dot{y}_d^2(t)) \end{aligned} \tag{7}$$

where atan2 is the four-quadrant inverse tangent operator. Then, it can be verified that $\mathbf{x}_d(t)$ satisfies the kinematic (1). Similarly, we assume $\mathbf{v}_d = [u_d, v_d, r_d]^{\mathrm{T}}$ obeys the dynamic (3), and the reference control forces $\boldsymbol{\tau}_d = [F_{ud}, F_{vd}, F_{rd}]^{\mathrm{T}}$ can be obtained by

$$\boldsymbol{\tau}_d = \mathbf{M}\dot{\mathbf{v}}_d + \mathbf{C}(\mathbf{v}_d)\mathbf{v}_d + \mathbf{D}(\mathbf{v}_d)\mathbf{v}_d + \mathbf{g}(\boldsymbol{\eta}_d) \tag{8}$$

where $\boldsymbol{\eta}_d = [x_d, y_d, \psi_d]^{\mathrm{T}}$ and $\dot{\mathbf{v}}_d$ can be calculated by taking the time derivative of (7). Furthermore, since P-5 is satisfied we take advantage of the Moore–Penrose pseudoinverse implementation to solve the TA subproblem and we can get the reference control for each thruster:

$$\mathbf{u}_d = (\mathbf{B}^{\mathrm{T}}\mathbf{B})^{-1}\mathbf{B}^{\mathrm{T}}\boldsymbol{\tau}_d = \mathbf{B}^{+}\boldsymbol{\tau}_d. \tag{9}$$

Proposition 1: Provided that *Assumption 1* holds and the reference signals are chosen as (7) then $\boldsymbol{\eta}_d$, $\dot{\boldsymbol{\eta}}_d$, and $\ddot{\boldsymbol{\eta}}_d$ are upper bounded, i.e., $\|\boldsymbol{\eta}_d(t)\|_\infty \leq \bar{\eta}_d$, $\|\dot{\boldsymbol{\eta}}_d(t)\|_\infty \leq \bar{\eta}_{d1}$ and $\|\ddot{\boldsymbol{\eta}}_d(t)\|_\infty \leq \bar{\eta}_{d2}$ for some positive numbers $\bar{\eta}_d$, $\bar{\eta}_{d1}$ and $\bar{\eta}_{d2}$.

Proof: With *Assumption 1*, we notice that the boundedness of $\boldsymbol{\eta}_d$, $\dot{\boldsymbol{\eta}}_d$, and $\ddot{\boldsymbol{\eta}}_d$ depends on the boundedness of ψ_d, $\dot{\psi}_d$ and $\ddot{\psi}_d$, respectively.

By definition, we have $|\psi_d| \leq \pi$. Since $\dot{\psi}_d = r_d$, we have $|\dot{\psi}_d| \leq \bar{p}_1\bar{p}_2/\underline{p_1^2}$. We explicit $\ddot{\psi}_d$ as follows:

$$\ddot{\psi}_d = \frac{\dot{x}_d\dddot{y}_d - \dot{y}_d\dddot{x}_d}{\dot{x}_d^2 + \dot{y}_d^2} - \frac{2(\dot{x}_d\ddot{x}_d + \dot{y}_d\ddot{y}_d)(\dot{x}_d\ddot{y}_d - \dot{y}_d\ddot{x}_d)}{(\dot{x}_d^2 + \dot{y}_d^2)^2}. \tag{10}$$

Obviously, we have $|\ddot{\psi}_d| \leq \bar{p}_1\bar{p}_3/\underline{p_1^2} + 2\bar{p}_1^2\bar{p}_2^2/\underline{p_1^2}$. Therefore, the bounds can be calculated by

$$\bar{\eta}_d = \max\{\bar{p}, \pi\} \tag{11a}$$

$$\bar{\eta}_{d1} = \max\{\bar{p}_1, \bar{p}_1\bar{p}_2/\underline{p_1^2}\} \tag{11b}$$

$$\bar{\eta}_{d2} = \max\{\bar{p}_2, \bar{p}_1\bar{p}_3/\underline{p_1^2} + 2\bar{p}_1^2\bar{p}_2^2/\underline{p_1^2}\}. \tag{11c}$$

■

Since $\dot{\boldsymbol{\eta}}_d = \mathbf{R}(\psi)\mathbf{v}_d$, together with P-6, (8) and (9), it can be easily shown that the reference state $\mathbf{x}_d$ and control $\mathbf{u}_d$ are also finite and upper bounded.

Then, an intuitive MPC formulation for the AUV trajectory tracking control can be established as follows:

$$\begin{aligned} \min_{\hat{\mathbf{u}}\in S(\delta)} \quad & J = \int_0^T \|\tilde{\mathbf{x}}(s)\|_Q^2 + \|\tilde{\mathbf{u}}(s)\|_R^2 ds + \|\tilde{\mathbf{x}}(T)\|_P^2 \\ \text{s.t.} \quad & \dot{\hat{\mathbf{x}}}(s) = \mathbf{f}(\hat{\mathbf{x}}(s), \hat{\mathbf{u}}(s)) \\ & \hat{\mathbf{x}}(0) = \mathbf{x}(t_0) \\ & |\hat{\mathbf{u}}(s)| \le \mathbf{u}_{\max} \end{aligned}$$

where $\hat{\mathbf{x}}(s)$ is the predicted state trajectory of the vehicle with respect to the predictive control $\hat{\mathbf{u}}(s)$, evolving from $\mathbf{x}(t_0)$ using the system model; $\tilde{\mathbf{x}} = \hat{\mathbf{x}} - \mathbf{x}_d$ is the error state and $\tilde{\mathbf{u}} = \hat{\mathbf{u}} - \mathbf{u}_d$ is the control error; $S(\delta)$ denotes the family of piecewise constant functions characterized by the sampling period δ and $T = N\delta$ is the prediction horizon; The weighting matrices Q, R, and P are positive definite.

However, it is well known that the closed-loop stability cannot be automatically guaranteed by the optimality of the solution due to the finite prediction horizon [25]. To ensure this important closed-loop property, complex offline design procedure should take place. For nonlinear systems, such as the AUV, with standard MPC design technique, local linearization needs to be performed in order to select appropriate weighting matrices and to construct an auxiliary local feedback control law. In this way, the ROA will be defined implicitly [26]. Besides, as mentioned in Section I, for the AUV tracking of a curve reference local linearization appears inappropriate.

To circumvent the local linearization while ensuring the closed-loop stability of the MPC tracking control, we exploit an auxiliary Lyapunov-based nonlinear tracking control law and formulate the LMPC problem by adding a contraction constraint to the original MPC formulation

$$\min_{\hat{\mathbf{u}}\in S(\delta)} \quad J = \int_0^T \|\tilde{\mathbf{x}}(s)\|_Q^2 + \|\hat{\mathbf{u}}(s)\|_R^2 ds + \|\tilde{\mathbf{x}}(T)\|_P^2 \tag{12a}$$

$$\text{s.t.} \quad \dot{\hat{\mathbf{x}}}(s) = \mathbf{f}(\hat{\mathbf{x}}(s), \hat{\mathbf{u}}(s)) \tag{12b}$$

$$\hat{\mathbf{x}}(0) = \mathbf{x}(t_0) \tag{12c}$$

$$|\hat{\mathbf{u}}(s)| \le \mathbf{u}_{\max} \tag{12d}$$

$$\frac{\partial V}{\partial \mathbf{x}}\mathbf{f}(\hat{\mathbf{x}}(0), \hat{\mathbf{u}}(0)) \le \frac{\partial V}{\partial \mathbf{x}}\mathbf{f}(\hat{\mathbf{x}}(0), h(\hat{\mathbf{x}}(0))) \tag{12e}$$

where $h(\cdot)$ is the auxiliary Lyapunov-based nonlinear tracking control law and $V(\cdot)$ is the corresponding Lyapunov function. The presence of contraction constraint (12e) allows us to show that the LMPC controller inherits the stability properties of the state feedback control $h(\mathbf{x})$ and a guaranteed ROA can be explicitly characterized. Furthermore, thanks to the online optimization procedure, the LMPC controller will automatically perform the best possible tracking control that respects the physical limitation of the system.

Algorithm 1: (LMPC Algorithm)

1: Input the objective function J in (12a);
2: Measure the current state $\mathbf{x}(t)$;
3: Solve the LMPC problem (12) with $\mathbf{x}(t_0) = \mathbf{x}(t)$, and let $\boldsymbol{\kappa}(s)$ denote the (sub-)optimal solution;
4: Implement $\boldsymbol{\kappa}(s)$ for only one sampling period: $\mathbf{u}(t) = \boldsymbol{\kappa}(s)$ for $s \in [0, \delta]$;
5: At next sampling time instant, set $t = t + \delta$, then repeat from step 2.

The LMPC-based trajectory tracking control will be implemented in the receding horizon fashion and the control algorithm is summarized in Algorithm 1.

Remark 1: As will be seen shortly in the following section, neither the recursive feasibility nor the closed-loop stability relies on the exact solution of the optimization. In Algorithm 1 suboptimal solutions are totally acceptable, which is highly desirable for any nonlinear MPC algorithm in view of the following facts. First, since the system dynamics are nonlinear, using iterative methods the best guaranteed solution to (12) is a local optimum. More importantly, for the implementation on embedded systems with limited computational resource, the iteration number may be restricted for real-time control. In other words, the compatibility with suboptimal solutions introduces the flexibility between numerical efficiency and control performance. We can easily make the tradeoff by specifying the maximum iteration number without destabilizing the tracking control.

IV. Stability Analysis

In this section, we first construct the auxiliary tracking controller using Lyapunov-based backstepping technique and then analyze the recursive feasibility and closed-loop stability of the LMPC under Algorithm 1.

A. Nonlinear BSC

To construct the contraction constraint in (12e), we need to find a state feedback controller together with the corresponding Lyapunov function. For the AUV trajectory tracking, the Lyapunov-based nonlinear controller can be designed via the backstepping technique.

Define the following change of variables:

$$\dot{\boldsymbol{\eta}}_r = \dot{\boldsymbol{\eta}}_d - \tilde{\boldsymbol{\eta}} \tag{13a}$$

$$\mathbf{v}_r = \mathbf{R}^{\mathrm{T}}(\psi)\dot{\boldsymbol{\eta}}_r \tag{13b}$$

$$\mathbf{s} = \dot{\boldsymbol{\eta}} - \dot{\boldsymbol{\eta}}_r = \dot{\tilde{\boldsymbol{\eta}}} + \tilde{\boldsymbol{\eta}} \tag{13c}$$

where $\tilde{\boldsymbol{\eta}} = \boldsymbol{\eta} - \boldsymbol{\eta}_d$ is the position tracking error. Considering the kinematic (1), we have

$$\dot{\boldsymbol{\eta}} - \dot{\boldsymbol{\eta}}_d = \mathbf{R}(\psi)(\mathbf{v} - \mathbf{v}_d). \tag{14}$$

We view $\mathbf{v}$ as a virtual control that stabilizes the trajectory tracking control

$$\mathbf{R}(\psi)\mathbf{v} = \mathbf{s} + \boldsymbol{\alpha}_1. \tag{15}$$

Choosing $\boldsymbol{\alpha}_1 = \dot{\boldsymbol{\eta}}_r$ and substituting it into (14) and (15) yields

$$\dot{\tilde{\boldsymbol{\eta}}} = \mathbf{s} + \boldsymbol{\alpha}_1 - \mathbf{R}(\psi)\mathbf{v}_d = -\tilde{\boldsymbol{\eta}} + \mathbf{s}. \tag{16}$$

Consider the following function:

$$V_1 = \frac{1}{2}\tilde{\boldsymbol{\eta}}^{\mathrm{T}}\mathbf{K}_p\tilde{\boldsymbol{\eta}} \tag{17}$$

where $\mathbf{K}_p = \mathbf{K}_p^{\mathrm{T}} > 0$ is a specified control gain matrix. Then, the time derivative of V_1 becomes

$$\dot{V}_1 = \tilde{\boldsymbol{\eta}}^{\mathrm{T}}\mathbf{K}_p\dot{\tilde{\boldsymbol{\eta}}} = -\tilde{\boldsymbol{\eta}}^{\mathrm{T}}\mathbf{K}_p\tilde{\boldsymbol{\eta}} + \mathbf{s}^{\mathrm{T}}\mathbf{K}_p\tilde{\boldsymbol{\eta}}. \tag{18}$$

Further construct the Lyapunov function candidate

$$V_2 = \frac{1}{2}\mathbf{s}^{\mathrm{T}}\mathbf{M}^*(\psi)\mathbf{s} + V_1 \tag{19}$$

where $\mathbf{M}^*(\psi) = \mathbf{R}(\psi)\mathbf{M}\mathbf{R}^{\mathrm{T}}(\psi)$.

Taking time derivative of V_2 results in

$$\dot{V}_2 = \mathbf{s}^{\mathrm{T}}\mathbf{M}^*(\psi)\dot{\mathbf{s}} + \tfrac{1}{2}\mathbf{s}^{\mathrm{T}}\dot{\mathbf{M}}^*(\psi)\mathbf{s} + \dot{V}_1. \tag{20}$$

Substituting the dynamic (3), we have

$$\begin{aligned}\dot{V}_2 = & -\mathbf{s}^{\mathrm{T}}[\mathbf{C}^*(\mathbf{v},\psi) + \mathbf{D}^*(\mathbf{v},\psi)]\mathbf{s} + \mathbf{s}^{\mathrm{T}}\mathbf{R}(\psi) \\ & \times [\boldsymbol{\tau} - \mathbf{M}\dot{\mathbf{v}}_r - \mathbf{C}(\mathbf{v})\mathbf{v}_r - \mathbf{D}(\mathbf{v})\mathbf{v}_r - \mathbf{g}(\boldsymbol{\eta})] \\ & + \frac{1}{2}\mathbf{s}^{\mathrm{T}}\dot{\mathbf{M}}^*(\psi)\mathbf{s} - \tilde{\boldsymbol{\eta}}^{\mathrm{T}}\mathbf{K}_p\tilde{\boldsymbol{\eta}} + \mathbf{s}^{\mathrm{T}}\mathbf{K}_p\tilde{\boldsymbol{\eta}}\end{aligned} \tag{21}$$

where $\mathbf{C}^*(\mathbf{v},\psi) = \mathbf{R}(\psi)[\mathbf{C}(\mathbf{v}) - \mathbf{M}\mathbf{R}^{\mathrm{T}}(\psi)\dot{\mathbf{R}}(\psi)]\mathbf{R}^{\mathrm{T}}(\psi)$ and $\mathbf{D}(\mathbf{v},\psi)^* = \mathbf{R}(\psi)\mathbf{D}(\mathbf{v})\mathbf{R}^{\mathrm{T}}(\psi)$.

By property P-2, it can be verified that

$$\mathbf{s}^{\mathrm{T}}(\dot{\mathbf{M}}^*(\psi) - 2\mathbf{C}^*(\mathbf{v},\psi))\mathbf{s} = 0 \ \ \forall \mathbf{v},\psi,\mathbf{s} \tag{22}$$

Therefore, if we choose the following control law:

$$\boldsymbol{\tau}(\mathbf{x}) = \mathbf{M}\dot{\mathbf{v}}_r + \mathbf{C}\mathbf{v}_r + \mathbf{D}\mathbf{v}_r + \mathbf{g} - \mathbf{R}^{\mathrm{T}}\mathbf{K}_p\tilde{\boldsymbol{\eta}} - \mathbf{R}^{\mathrm{T}}\mathbf{K}_d\mathbf{s} \tag{23}$$

where $\mathbf{K}_d > 0$ is another user specified control gain matrix, the (21) becomes

$$\dot{V}_2 = -\mathbf{s}^{\mathrm{T}}[\mathbf{D}^*(\mathbf{v},\psi) + \mathbf{K}_d]\mathbf{s} - \tilde{\boldsymbol{\eta}}^{\mathrm{T}}\mathbf{K}_p\tilde{\boldsymbol{\eta}}. \tag{24}$$

By property P-4, we have $\dot{V}_2 \le 0$. Then, by standard Lyapunov arguments the closed-loop system under (23) is globally asymptotically stable with respect to the equilibrium $[\tilde{\boldsymbol{\eta}}, \mathbf{s}] = [\mathbf{0}, \mathbf{0}]$.

Therefore, the detailed expression of the contraction constraint (12e) corresponding to (23) is

$$\begin{aligned}&-\hat{\mathbf{s}}(0)^{\mathrm{T}}\mathbf{D}^*(\hat{\mathbf{v}}(0),\hat{\psi}(0))\hat{\mathbf{s}}(0) + \hat{\mathbf{s}}(0)^{\mathrm{T}}\mathbf{R}(\hat{\psi}(0))[\mathbf{B}\hat{\mathbf{u}}(0) \\ &\quad -\mathbf{M}\dot{\hat{\mathbf{v}}}_r(0) - \mathbf{C}(\hat{\mathbf{v}}(0))\hat{\mathbf{v}}_r(0) - \mathbf{D}(\hat{\mathbf{v}}(0))\hat{\mathbf{v}}_r(0) \\ &\quad -\mathbf{g}(\hat{\boldsymbol{\eta}}(0))] - \tilde{\boldsymbol{\eta}}(0)^{\mathrm{T}}\mathbf{K}_p\tilde{\boldsymbol{\eta}}(0) + \hat{\mathbf{s}}(0)^{\mathrm{T}}\mathbf{K}_p\tilde{\boldsymbol{\eta}}(0) \\ &\le -\hat{\mathbf{s}}(0)^{\mathrm{T}}[\mathbf{D}^*(\hat{\mathbf{v}}(0),\hat{\psi}(0)) + \mathbf{K}_d]\hat{\mathbf{s}}(0) - \tilde{\boldsymbol{\eta}}(0)^{\mathrm{T}}\mathbf{K}_p\tilde{\boldsymbol{\eta}}(0).\end{aligned} \tag{25}$$

Note that, here, we construct the contraction constraint with the help of the auxiliary nonlinear backstepping controller. However, in principle, any other Lyapunov-based tracking controller can be used.

B. Stability Analysis for the LMPC

Now, we analyze the recursive feasibility of the problem (12) and the closed-loop stability under Algorithm 1.

For simplicity, we make the following assumption.

Assumption 2: All the thrusters have the same capacity, i.e., $|u_i| \le u_{\max}$.

Indeed, the above assumption is satisfied with the Falcon. Then, we can have the following results.

Proposition 2: Consider the TA using the Moore–Penrose pseudoinverse solution, i.e., $\mathbf{u} = \mathbf{B}^+\boldsymbol{\tau}$ and specify the maximum possible generalized thrust force by $\tau_{\max} = \|\boldsymbol{\tau}_{\max}\|_\infty$ with $\boldsymbol{\tau}_{\max} = [F_{u,\max}, F_{v,\max}, F_{r,\max}]^{\mathrm{T}}$.

If the following relation holds

$$\tau_{\max} \le \frac{u_{\max}}{\bar{b}^+} \tag{26}$$

where $\bar{b}^+ = \|\mathbf{B}^+\|_\infty$, then the TA is always feasible, i.e., $\|\mathbf{u}\|_\infty \le u_{\max}$.

Proof: Taking infinity norm on both sides of $\mathbf{u} = \mathbf{B}^+\boldsymbol{\tau}$ we have

$$\|\mathbf{u}\|_\infty = \|\mathbf{B}^+\boldsymbol{\tau}\|_\infty \le \bar{b}^+\|\boldsymbol{\tau}\|_\infty \le \bar{b}^+\tau_{\max}. \tag{27}$$

Having (26) and *Assumption 2*, it follows

$$\|\mathbf{u}\|_\infty \le \bar{b}^+\tau_{\max} \le u_{\max}. \tag{28}$$

Lemma 1: Provided that the AUV is controlled by the backstepping controller (23), the Coriolis and centripetal matrix $\mathbf{C}(\mathbf{v})$ and damping matrix $\mathbf{D}(\mathbf{v})$ are bounded satisfying

$$\|\mathbf{C}(\mathbf{v})\|_\infty \le \bar{c} = 2\sqrt{2}\bar{m}\bar{\eta}_{d1} + 4\sqrt{2}\bar{m}\|\gamma(0)\|_2 \tag{29}$$

$$\|\mathbf{D}(\mathbf{v})\|_\infty \le \bar{d} = \bar{d}_1 + \bar{d}_2\left(\sqrt{2}\bar{\eta}_{d1} + 2\sqrt{2}\|\gamma(0)\|_2\right) \tag{30}$$

where $\gamma(t) = col(\tilde{\boldsymbol{\eta}}(t), \mathbf{s}(t))$, $\bar{d}_1 = \max\{|X_u|, |Y_v|, |N_r|\}$ and $\bar{d}_2 = \max\{D_u, D_v, D_r\}$.

Proof: Define $\gamma' = col(\tilde{\boldsymbol{\eta}}, \mathbf{R}^{\mathrm{T}}(\psi)\mathbf{s})$ and we can reformulate the Lyapunov function (19) as $V_2 = \frac{1}{2}\gamma'^{\mathrm{T}}\Pi\gamma'$ with $\Pi = \mathrm{diag}(\mathbf{K}_p, \mathbf{M})$. Since $\dot{V}_2 \le 0$, we have $\|\gamma'(t)\|_2 \le \|\gamma'(0)\|_2$. Furthermore, by P-3 we have $\|\gamma'(t)\|_2 = \|\gamma(t)\|_2$ followed by

$$\|\gamma(t)\|_2 \le \|\gamma(0)\|_2. \tag{31}$$

By definition, we have $\|\tilde{\boldsymbol{\eta}}\|_\infty \le \|\gamma\|_\infty$ and $\|\mathbf{s}\|_\infty \le \|\gamma\|_\infty$. Then, the following can hold

$$\|\dot{\tilde{\boldsymbol{\eta}}}\|_\infty = \|\mathbf{s} - \tilde{\boldsymbol{\eta}}\|_\infty \le \|\mathbf{s}\|_\infty + \|\tilde{\boldsymbol{\eta}}\|_\infty \le 2\|\gamma\|_\infty. \tag{32}$$

Considering that $\|\gamma\|_\infty \le \|\gamma\|_2$, we have

$$\|\dot{\tilde{\boldsymbol{\eta}}}(t)\|_\infty \le 2\|\gamma(0)\|_2. \tag{33}$$

Since $\|\dot{\boldsymbol{\eta}}\|_\infty = \|\dot{\boldsymbol{\eta}}_d + \dot{\tilde{\boldsymbol{\eta}}}\|_\infty \le \|\dot{\boldsymbol{\eta}}_d\|_\infty + \|\dot{\tilde{\boldsymbol{\eta}}}\|_\infty$, together with (33) and *Proposition 1*, it follows that

$$\|\dot{\boldsymbol{\eta}}(t)\|_\infty \le \bar{\eta}_{d1} + 2\|\gamma(0)\|_2. \tag{34}$$

By (1) and P-3, we have $\|\mathbf{v}\|_\infty = \|\mathbf{R}^{\mathrm{T}}(\psi)\dot{\boldsymbol{\eta}}\|_\infty \le \sqrt{2}\|\dot{\boldsymbol{\eta}}\|_\infty$ due to the fact that $\|\mathbf{R}^{\mathrm{T}}(\psi)\|_\infty = \max\{|\cos\psi| + |\sin\psi|, 1\} \le \sqrt{2}$. Therefore, the following holds

$$\|\mathbf{v}(t)\|_\infty \le \sqrt{2}\bar{\eta}_{d1} + 2\sqrt{2}\|\gamma(0)\|_2. \tag{35}$$

Taking infinity norm on (4) and substituting (35), together with P-1 we can have (29) and similarly (30). ■

Theorem 1: Suppose the control gain matrices are chosen as $\mathbf{K}_p = \text{diag}\{k_{pi}\}$ and $\mathbf{K}_d = \text{diag}\{k_{di}\}$, positive definite. Let $\bar{k}_p = \max\{k_{pi}\}$ denote the largest element in $\mathbf{K}_p$ and $\bar{k}_d = \max\{k_{di}\}$ denote the largest element in $\mathbf{K}_d$. Suppose *Assumption 1* and *Assumption 2* can hold. For $h(\mathbf{x}) = \mathbf{B}^+\boldsymbol{\tau}(\mathbf{x})$, if the following relation can be satisfied

$$\bar{m}\bar{v}_{r1} + (\bar{c}+\bar{d})\bar{v}_r + \bar{g} + \sqrt{2}(\bar{k}_p + \bar{k}_d)\|\gamma(0)\|_2 \le \tau_{\max} \quad (36)$$

with $\bar{v}_{r1} = \sqrt{2}\bar{\eta}_{d2} + 2\bar{\eta}_{d1}^2 + (2\sqrt{2} + 6\bar{\eta}_{d1})\|\gamma(0)\|_2 + 4\|\gamma(0)\|_2^2$ and $\bar{v}_r = \sqrt{2}(\bar{\eta}_{d1} + \|\gamma(0)\|_2)$, and $\tau_{\max}$ follows (26), then the LMPC (12) admits recursive feasibility, i.e., $|h(\hat{\mathbf{x}}(t))| \le \mathbf{u}_{\max}$ for all $t \ge 0$ where $\mathbf{u}_{\max} = u_{\max}\mathbf{1}$.

Proof: We notice that given the current system state $\mathbf{x}(t)$, $h(\hat{\mathbf{x}})$ is always feasible for the LMPC problem (12) if $|h(\hat{\mathbf{x}})| \le \mathbf{u}_{\max}$ can be satisfied.

Since we have *Proposition 1* and the fact that $\|\hat{\dot{\boldsymbol{\eta}}}\|_\infty \le \|\hat{\gamma}\|_\infty \le \|\gamma(0)\|_2$, it can be verified that $\|\hat{\mathbf{v}}_r\|_\infty \le \bar{v}_r$ with $\bar{v}_r = \sqrt{2}(\bar{\eta}_{d1} + \|\gamma(0)\|_2)$ by taking infinity norm on (13).

Taking time derivative on both sides of (13a) and (13b) we have

$$\begin{aligned}\dot{\mathbf{v}}_r &= \mathbf{R}^{\mathrm{T}}(\psi)\ddot{\boldsymbol{\eta}}_r - \dot{\psi}\boldsymbol{\Omega}(\psi)\dot{\boldsymbol{\eta}}_r \\ &= \mathbf{R}^{\mathrm{T}}(\psi)(\ddot{\boldsymbol{\eta}}_d - \dot{\tilde{\boldsymbol{\eta}}}) - r\boldsymbol{\Omega}(\psi)(\dot{\boldsymbol{\eta}}_d - \tilde{\boldsymbol{\eta}})\end{aligned} \quad (37)$$

where

$$\boldsymbol{\Omega}(\psi) = \begin{bmatrix}\sin\psi & -\cos\psi & 0\\ \cos\psi & \sin\psi & 0\\ 0 & 0 & 0\end{bmatrix} \quad (38)$$

which admits $\|\boldsymbol{\Omega}(\psi)\|_\infty \le \sqrt{2}$. Then taking infinity norm on (37) and combining (33) and (35), we can have $\|\dot{\hat{\mathbf{v}}}_r\|_\infty \le \bar{v}_{r1}$ with $\bar{v}_{r1} = \sqrt{2}\bar{\eta}_{d2} + 2\bar{\eta}_{d1}^2 + (2\sqrt{2} + 6\bar{\eta}_{d1})\|\gamma(0)\|_2 + 4\|\gamma(0)\|_2^2$.

Then taking infinity norm on both sides of (23), together with *Lemma 1* and P-6 we have

$$\|\boldsymbol{\tau}(\hat{\mathbf{x}})\|_\infty \le \bar{m}\bar{v}_{r1} + (\bar{c}+\bar{d})\bar{v}_r + \bar{g} + \sqrt{2}(\bar{k}_p + \bar{k}_d)\|\gamma(0)\|_2 \quad (39)$$

If (36) can be satisfied, then $\|\boldsymbol{\tau}(\hat{\mathbf{x}})\|_\infty \le \tau_{\max}$ can hold. With (26), we can guarantee that $\|h(\hat{\mathbf{x}}(s))\|_\infty \le u_{\max}$ can be satisfied all the time.

Note that the nonlinear backstepping controller acts as an initial guess for the optimization problem (12), but is never applied to the system. As a result, the feasibility is guaranteed by the auxiliary controller and the control performance will be optimized by the LMPC controller.

Theorem 2: Suppose *Assumption 1* and *Assumption 2* can hold, then the closed-loop system under Algorithm 1 is asymptotically stable with respect to the equilibrium $[\tilde{\boldsymbol{\eta}}, \mathbf{s}] = [\mathbf{0}, \mathbf{0}]$, i.e., the AUV will converge to the desired trajectory $p(t)$ with the LMPC-based trajectory tracking control.

Proof: Since we have the Lyapunov function $V_2(\mathbf{x})$ in (19), continuously differentiable and radically unbounded, by converse Lyapunov theorems [27], there exist functions $\beta_i(\cdot)$, $i = 1, 2, 3$ which belong to class $\mathcal{K}_\infty$ such that the following inequalities hold:

$$\beta_1(\|\mathbf{x}\|) \le V_2(\mathbf{x}) \le \beta_2(\|\mathbf{x}\|) \quad (40a)$$

$$\frac{\partial V}{\partial \mathbf{x}}\mathbf{f}(\mathbf{x}, h(\mathbf{x})) \le -\beta_3(\|\mathbf{x}\|). \quad (40b)$$

Considering (12e) and that the optimal solution $\boldsymbol{\kappa}(s)$ will be implemented for one sampling period each time, we have

$$\frac{\partial V}{\partial \mathbf{x}}\mathbf{f}(\mathbf{x}, \mathbf{u}(\mathbf{x})) \le \frac{\partial V}{\partial \mathbf{x}}\mathbf{f}(\mathbf{x}, h(\mathbf{x})) \le -\beta_3(\|\mathbf{x}\|). \quad (41)$$

By Lyapunov arguments (Theorem 4.8 in [27]) we claim that the closed-loop system under Algorithm 1 is asymptotically stable with a guaranteed ROA

$$\mathcal{X} = \{\mathbf{x} \in \mathbb{R}^n \mid (36)\}. \quad (42)$$

Furthermore, $\mathcal{X}$ can be enlarged by shrinking the magnitude of the control gains $\bar{k}_p$ and $\bar{k}_d$.

Remark 2: Although the asymptotical stability relies only on the positive definiteness of the control gain matrices $\mathbf{K}_p$ and $\mathbf{K}_d$, the tracking control performance with the backstepping controller $\boldsymbol{\tau}(\mathbf{x})$ is determined by the magnitude of the control gains. From (24), we can see that smaller values of $\bar{k}_p$ and $\bar{k}_d$ result in slower convergence. However, for the proposed LMPC-based trajectory tracking control, thanks to the optimization procedure, the controller can automatically make full use of the thrust capability to generate the best possible tracking control with respect to the objective function (12a) even if we have selected small control gains for a large ROA.

V. Simulation Results

In this section, we provide the simulation results of the AUV tracking control which highlight the advantages of the proposed LMPC method. All the simulations are based on the experimentally identified dynamic model of the Falcon [28].

A. Parameter Selection

Two desired trajectories are used to test the AUV tracking control. The first one (Case I) is a sinusoidal trajectory defined as follows:

$$p(t) = \begin{cases} x_d = 0.5t \\ y_d = \sin(0.5t) \end{cases} \quad (43)$$

and the second one (Case II) is an eight-shaped trajectory defined by

$$p(t) = \begin{cases} x_d = -\sin(0.5t) \\ y_d = \sin(0.25t) \end{cases}. \quad (44)$$

For the LMPC controller, the following parameters are used: the sampling period is $\delta = 0.1$ [sec]; the prediction horizon is $T = 5\delta$; the weighting matrices are chosen as $Q = \text{diag}(10^5, 10^5, 10^3, 10^2, 10^2, 10^2)$, $R = \text{diag}(10^{-4}, 10^{-4}, 10^{-4}, 10^{-4})$ and $P = \text{diag}(10^3, 10^3, 10^2, 10, 10, 10)$; and the limit on each thruster is 500 [N]. The control gains $\mathbf{K}_p = \mathbf{K}_d = \text{diag}(1, 1, 1)$. The initial condition is $\mathbf{x}(0) = [0.5, 0, 0, 0, 0, 0]^{\mathrm{T}}$.

To solve the LMPC problem (12) numerically, we need to discretize the problem and then solve the corresponding

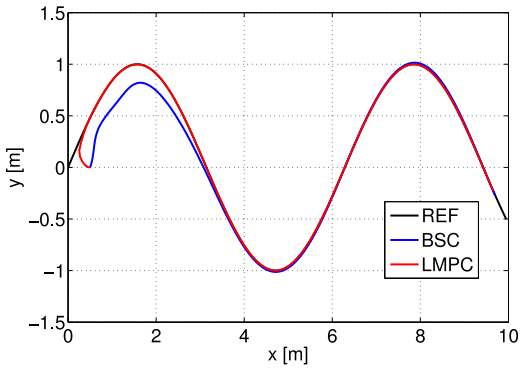

Fig. 2. AUV trajectory in *xoy* plane—Case I.

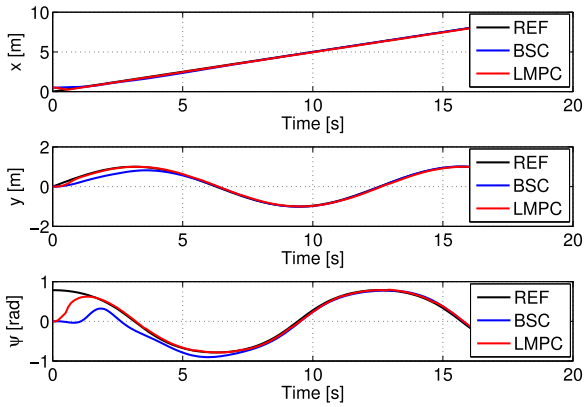

Fig. 3. State trajectories—Case I.

Karush–Kuhn–Tucker conditions by the sequential quadratic programming method [29].

B. Tracking Performance

The trajectory tracking results for Case I are shown in Figs. 2 and 3. The blue curve is the simulated AUV trajectories using backstepping control (BSC), and the red curve is the AUV trajectories with the proposed LMPC control, while the black curve is the desired sinusoidal trajectory. As we can see, both BSC and LMPC drive the vehicle to the desired trajectory, which verifies the closed-loop stability. But obviously the LMPC controller generates a much faster convergence than the BSC controller. This is because we have selected small control gain matrices $\mathbf{K}_p$ and $\mathbf{K}_d$ for a large ROA. The simulation results demonstrate the enhanced tracking control performance brought by the online optimization.

The required control forces for each thruster are plotted in Fig. 4. We observe that in the beginning of the tracking, the LMPC controller fully uses the onboard thrust capability in order to generate the fastest possible convergence while respecting the physical limit of thrusters. In other words, the magnitude of control commands stay within the permitted range as expected.

The simulation results for Case II are provided through Figs. 5–7. Similar observations can be made: the AUV converges faster to the desired trajectory when adopting the proposed LMPC-based tracking control and the calculated control commands are always feasible for the real system.

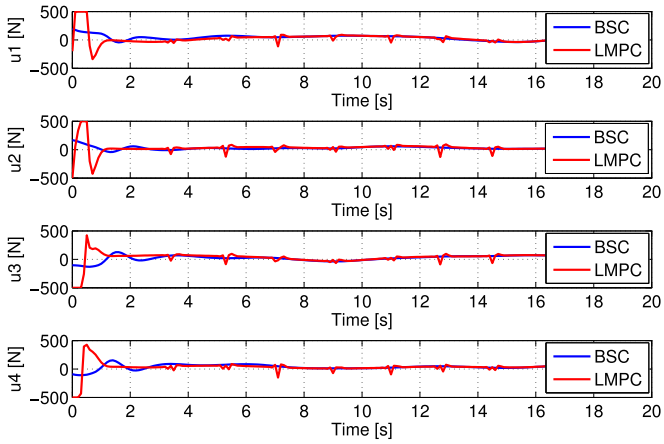

Fig. 4. Control input signals—Case I.

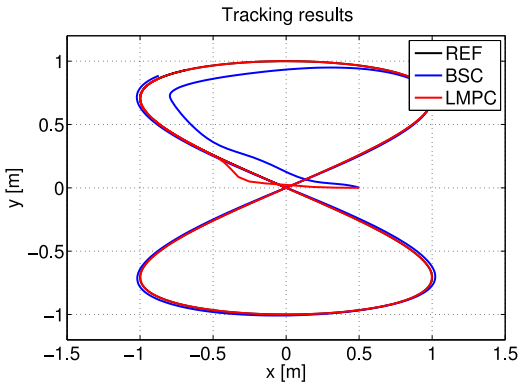

Fig. 5. AUV trajectory in *xoy* plane—Case II.

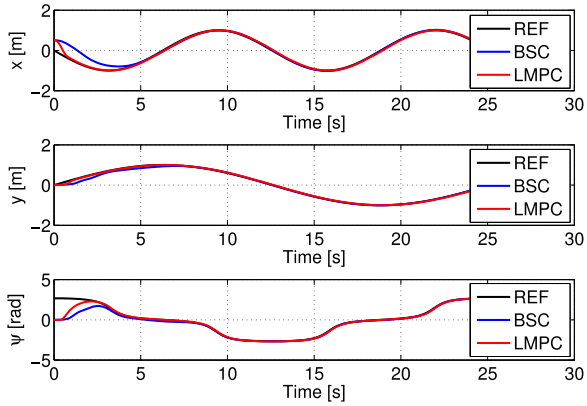

Fig. 6. State trajectories—Case II.

C. Robust Test

The receding horizon implementation introduces feedback into the closed-loop system, and an additional merit about the LMPC tracking control is the inherent robustness to uncertainties and disturbances [30], which is perfect for marine control systems. In the simulations, the robustness of the

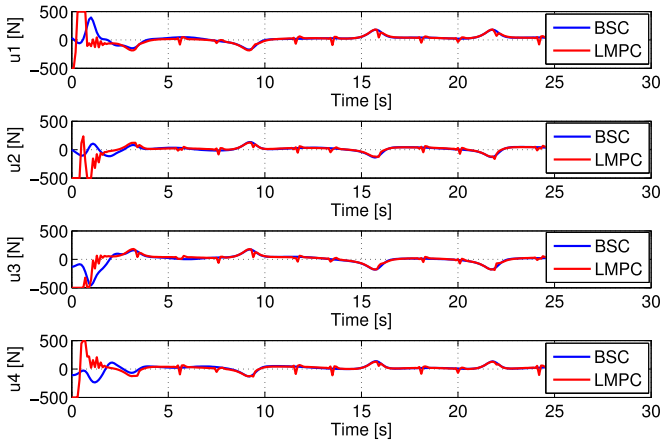

Fig. 7. Control input signals—Case II.

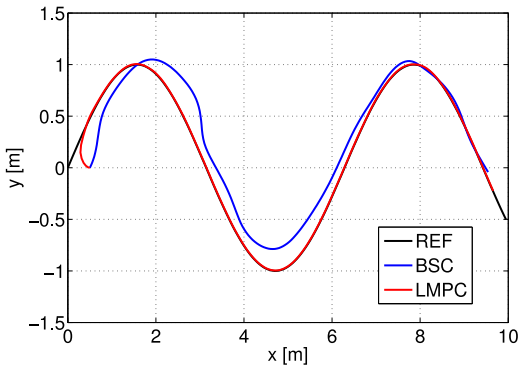

Fig. 8. AUV trajectory in *xoy* plane with disturbance—Case I.

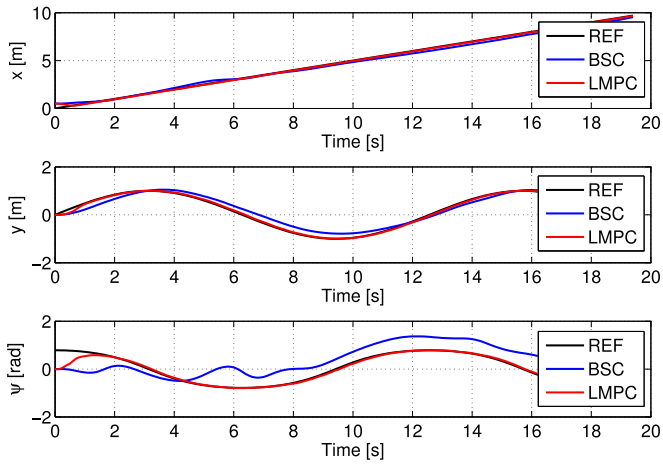

Fig. 9. State trajectories with disturbance—Case I.

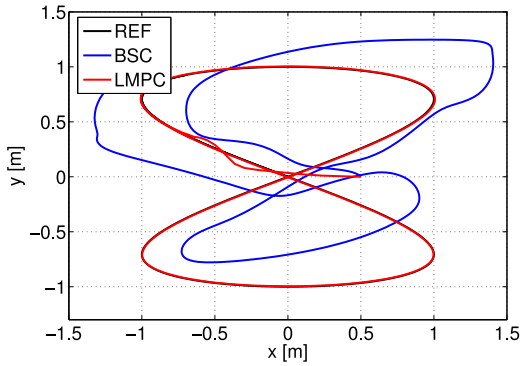

Fig. 10. AUV trajectory in *xoy* plane with disturbance—Case II.

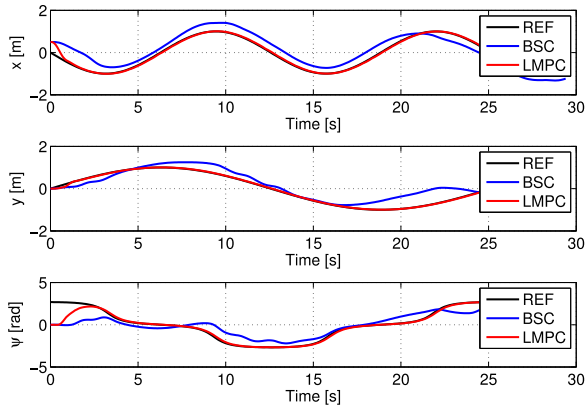

Fig. 11. State trajectories with disturbance—Case II.

TABLE I
MSE WITH DISTURBANCES—CASE I

MSE	Backstepping	LMPC	Improvement
x [m^2]	0.0418	0.0052	87.5%
y [m^2]	0.0297	0.0015	94.9%
ψ [rad^2]	0.3207	0.0184	94.3%

TABLE II
MSE WITH DISTURBANCES—CASE II

MSE	Backstepping	LMPC	Improvement
x [m^2]	0.1483	0.0059	96.0%
y [m^2]	0.0977	0.0005	99.5%
ψ [rad^2]	1.0081	0.2480	75.4%

tracking control is also investigated. To show the robustness of the BSC and LMPC, we simulate the AUV tracking control under very strict test condition: there exists a 30% model parameter error and an ocean current introduced disturbance of magnitude $[100(N), 100(N), 0(Nm)]^{\mathrm{T}}$.

From the simulation results illustrated in Figs. 8–11, we find that the LMPC-based tracking control still leads the AUV well converged to the desired trajectory, while the tracking control with BSC exists large tracking errors. The mean square errors (MSE) for both cases are summarized in Tables I and II. Roughly, the MSEs are more than 20 times smaller with the LMPC than that with BSC especially for Case II. This is because LMPC can leverage online optimization to schedule an appropriate control gain to well compensate the disturbances while BSC is a fixed gain controller and lacks such flexibility. The robustness of trajectory tracking control, therefore, is significantly improved by the LMPC control.

VI. Conclusion

In this paper, we have presented a novel LMPC algorithm for the trajectory tracking control of an AUV. By incorporating online optimization into the existing Lyapunov-based tracking controller, the control performance as well as the robustness can be largely enhanced. Besides, the TA subproblem need not be considered separately since the optimization essentially allows it to be solved simultaneously with the LMPC controller design. The recursive feasibility and closed-loop stability of the LMPC control are rigorously proved. Simulation results of tracking different trajectories revealed the advantages of the proposed LMPC-based trajectory tracking control.

In the near future, experiments on the Saab SeaEye Falcon will be conducted to verify the proposed LMPC method. Also, we are interested in improving the closed-loop property of LMPC tracking control system by incorporating salient features of other control methods such as sliding mode control [31], robust control [13], and fuzzy-model-based control [17].

References

[1] Y. Shi, C. Shen, H. Fang, and H. Li, "Advanced control in marine mechatronic systems: A survey," *IEEE/ASME Trans. Mechatronics*, vol. 22, no. 3, pp. 1121–1131, Jun. 2017.

[2] H. Li, P. Xie, and W. Yan, "Receding horizon formation tracking control of constrained underactuated autonomous underwater vehicles," *IEEE Trans. Ind. Electron.*, vol. 64, no. 6, pp. 5004–5013, Jun. 2017.

[3] J. Gao, A. Proctor, Y. Shi, and C. Bradley, "Hierarchical model predictive image-based visual servoing of underwater vehicles with adaptive neural network dynamic control," *IEEE Trans. Cybern.*, vol. 46, no. 10, pp. 2323–2334, Oct. 2016.

[4] Z. Peng, J. Wang, and D. Wang, "Distributed containment maneuvering of multiple marine vessels via neurodynamics-based output feedback," *IEEE Trans. Ind. Electron.*, vol. 64, no. 5, pp. 3831–3839, May. 2017.

[5] T. Fossen, *Marine Control Systems: Guidance, Navigation and Control of Ships, Rigs and Underwater Vehicles*. Trondheim, Norway: Marine Cybernetics, 2002.

[6] F. Repoulias and E. Papadopoulos, "Plannar trajectory planning and tracking control design for underactuated AUVs," *Ocean Eng.*, vol. 34, nos. 11/12, pp. 1650–1667, Aug. 2007.

[7] K. Do, Z. Jiang, J. Pan, and H. Nijmeijer, "A global output-feedback controller for stabilization and tracking of underactuated ODIN: A spherical underwater vehicle," *Automatica*, vol. 40, pp. 117–124, 2004.

[8] S. Soylu, A. Proctor, R. Podhorodeski, C. Bradley, and B. Buckham, "Precise trajectory control for an inspection class ROV," *Ocean Eng.*, vol. 111, no. 1, pp. 508–523, Jan. 2015.

[9] S. Soylu, B. Buckham, and R. Podhorodeski, "A chattering-free sliding-mode controller for underwater vehicles with fault-tolerant infinity-norm thrust allocation," *Ocean Eng.*, vol. 35, no. 16, pp. 1647–1659, Nov. 2008.

[10] T. Salgado-Jimenez, J. Spiewak, P. Fraisse, and B. Jouvencel, "A robust control algorithm for AUV: Based on a high order sliding mode," in *Proc. MTS/IEEE Techno-Oceans*, Kobe, Japan, 2004, pp. 276–281.

[11] H. Zhang and J. Wang, "Active steering actuator fault detection for an automatically-steered electric ground vehicle," *IEEE Trans. Veh. Technol.*, vol. 66, no. 5, pp. 3685–3702, May. 2017.

[12] H. Zhang and J. Wang, "Adaptive sliding-mode observer design for a selective catalytic reduction system of ground-vehicle diesel engines," *IEEE/ASME Trans. Mechatronics*, vol. 21, no. 4, pp. 2027–2038, Aug. 2016.

[13] H. Zhang, G. Zhang, and J. Wang, "H_∞ observer design for LPV systems with uncertain measurements on scheduling variables: Application to an electric ground vehicle," *IEEE/ASME Trans. Mechatronics*, vol. 21, no. 3, pp. 1659–1670, Jun. 2016.

[14] D. Mayne, J. Rawlings, C. Rao, and P. Scokaert, "Constrained model predictive control: Stability and optimality," *Automatica*, vol. 36, no. 6, pp. 789–841, Jun. 2000.

[15] H. Li and Y. Shi, *Robust Receding Horizon Control for Networked and Distributed Nonlinear Systems* (Studies in Systems, Decision and Control). New York, NY, USA: Springer, 2016.

[16] Y. Wei, J. Qiu, H. Karimi, and M. Wang, "New results on H_∞ dynamic output feedback control for Markovian jump systems with time-varying delay and defective mode information," *Opt. Control Appl. Methods*, vol. 35, no. 6, pp. 656–675, Nov. 2014.

[17] Y. Wei, J. Qiu, and H. Karimi, "Reliable output feedback control of discrete-time fuzzy affine systems with actuator faults," *IEEE Trans. Circuits Syst. I*, vol. 64, no. 1, pp. 170–181, Jan. 2017.

[18] S. Qin and T. Badgwell, "An overview of nonlinear model predictive control applications," in *Nonlinear Model Predictive Control*, Cambridge, MA, USA: Birkhauser, 2000, pp. 369–392.

[19] H. Li, Y. Shi, and W. Yan, "On neighbor information utilization in distributed receding horizon control for consensus-seeking," *IEEE Trans. Cybern.*, vol. 46, no. 9, pp. 2019–2027, Sep. 2016.

[20] W. Naeem, R. Sutton, and S. Ahmad, "Pure pursuit guidance and model predictive control of an autonomous underwater vehicle for cable/pipeline tracking," in *Proc. World Maritime Technol. Conf.*, San Francisco, CA, USA, 2003, pp. 1–15.

[21] C. Shen, Y. Shi, and B. Buckham, "Integrated path planning and tracking control of an AUV: A unified receding horizon optimization approach," *IEEE/ASME Trans. Mechatronics*, vol. 22, no. 3, pp. 1163–1173, Jun. 2017.

[22] C. Shen, Y. Shi, and B. Buckham, "Modified C/GMRES algorithm for fast nonlinear model predictive tracking control of AUVs," *IEEE Trans. Control Syst. Technol.*, vol. 25, no. 5, pp. 1896–1904, Sep. 2017.

[23] C. Shen, Y. Shi, and B. Buckham, "Nonlinear model predictive control for trajectory tracking of an AUV: A distributed implementation," in *Proc. IEEE Conf. Decision. Control*, Las Vegas, NV, USA, Dec. 2016, pp. 5998–6003.

[24] P. Christofides, J. Liu, and D. Munoz de la Pena, *Networked and Distributed Predictive Control: Methods and Nonlinear Process Network Applications*. London, U.K: Springer, 2011.

[25] D. Mayne, "Model predictive control: Recent developments and future promise," *Automatica*, vol. 50, pp. 2967–2986, 2014.

[26] J. Rawlings and D. Mayne, *Model Predictive Control: Theory and Design*. Madison, WI, USA: Nob Hill Publishing, 2009.

[27] H. Khalil, *Nonlinear Systems*. New York, NY, USA: Prentice-Hall, 1996.

[28] A. Proctor, "Semi-automous guidance and control of a Saab SeaEye Falcon ROV," Ph.D. dissertation, University of Victoria, Victoria, BC, 2014.

[29] A. Antoniou and W. Lu, *Practical Optimization: Algorithms and Engineering Applications*. New York, NY, USA: Springer, 2007.

[30] G. Pannocchia, J. Rawlings, and S. Wright, "Inherently robust suboptimal nonlinear MPC: Theory and application," in *Proc. IEEE 50th Conf. Decision Control Eur. Control Conf.*, Orlando, FL, USA, 2011, pp. 3398–3403.

[31] M. Rubagotti, D. Raimondo, A. Ferrara, and L. Magni, "Robust model predictive control with integral sliding mode in continuous-time sampled-data nonlinear systems," *IEEE Trans. Autom. Control*, vol. 56, no. 3, pp. 556–570, Mar. 2011.

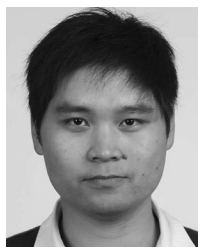

Chao Shen (M'16) received the B.Eng. degree in automation engineering and the M.A.Sc. degree in control science and engineering from Northwestern Polytechnical University, Xi'an, China, in 2009 and 2012, respectively. Since 2012, he has been working toward the Ph.D. degree in mechanical engineering at the Applied Control and Information Processing Laboratory, University of Victoria, Victoria, BC, Canada.

His current research interests include model predictive control, optimization and optimal control, modeling and control of ocean robotics, and nonlinear system control.

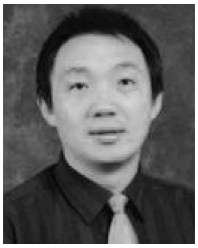

Yang Shi (SM'09–F'17) received the Ph.D. degree in electrical and computer engineering from the University of Alberta, Edmonton, AB, Canada, in 2005.

From 2005 to 2009, he was a Faculty Member with the Department of Mechanical Engineering, University of Saskatchewan, Saskatoon, SK, Canada. He is currently a Professor with the Department of Mechanical Engineering, University of Victoria, Victoria, BC, Canada. His current research interests include networked and distributed systems, model predictive control, industrial cyber-physical systems, mechatronics, and energy systems.

Dr. Shi received the University of Saskatchewan Student Union Teaching Excellence Award in 2007 and the Faculty of Engineering Teaching Excellence Award at the University of Victoria in 2012. He received the JSPS Invitation Fellowship (short-term) in 2013 and the 2015 Craigdarroch Silver Medal for Excellence in Research at the University of Victoria. He is currently a Co-Editor-in-Chief of the IEEE TRANSACTIONS ON INDUSTRIAL ELECTRONICS. He is also an Associate Editor for *Automatica*, IEEE TRANSACTIONS ON CONTROL SYSTEMS TECHNOLOGY, IEEE/ASME TRANSACTIONS ON MECHATRONICS, and *ASME Journal of Dynamic Systems, Measurement, and Control*. He is a Fellow of the Canadian Society for Mechanical Engineering, a Fellow of the American Society of Mechanical Engineers, and a registered Professional Engineer in British Columbia, Canada.

Brad Buckham (M'06) received the Ph.D degree in mechanical engineering from the University of Victoria (UVic), Victoria, BC, Canada, in 2003.

Currently, he is an Associate Professor in the Department of Mechanical Engineering at the Univeristy of Victoria. He joined UVic in 2003 and since that time has established a research program that is focused on the dynamics, simulation and control of cabled ocean systems such as towed vehicles, tethered remotely operated vehicle-manipulators, and moored wave and wind energy converters.

Dr. Buckham is a member of the IEEE Oceanic Engineering Society, the International Society of Offshore and Polar Engineers and is a registered Professional Engineer in British Columbia Canada.